Size fractions of organic matter pools influence their stability : Application of the Rock-Eval ® analysis to beech forest soils

David Sebag, Eric P. Verrecchia, Thierry Adatte, Michaël Aubert, Guillaume Cailleau, Thibaud Decaëns, Isabelle Kowalewski, Jean Trap, Fabrice Bureau, Mickael Hedde

▶ **To cite this version:**

David Sebag, Eric P. Verrecchia, Thierry Adatte, Michaël Aubert, Guillaume Cailleau, et al.. Size fractions of organic matter pools influence their stability : Application of the Rock-Eval ® analysis to beech forest soils. Pedosphere, 2022, 32 (4), pp.565-575. 10.1016/S1002-0160(21)60050-4 . hal-03704212

HAL Id: hal-03704212
https://ifp.hal.science/hal-03704212

Submitted on 24 Jun 2022

HAL is a multi-disciplinary open access archive for the deposit and dissemination of scientific research documents, whether they are published or not. The documents may come from teaching and research institutions in France or abroad, or from public or private research centers.

L'archive ouverte pluridisciplinaire **HAL**, est destinée au dépôt et à la diffusion de documents scientifiques de niveau recherche, publiés ou non, émanant des établissements d'enseignement et de recherche français ou étrangers, des laboratoires publics ou privés.

Size fractions of organic matter pools influence their stability: Application of the Rock-Eval® analysis to beech forest soils

David SEBAG[1,2,3,*], Eric P. VERRECCHIA[2], Thierry ADATTE[4], Michaël AUBERT[5], Guillaume CAILLEAU[6], Thibaud DECAËNS[7], Isabelle KOWALEWSKI[3], Jean TRAP[8], Fabrice BUREAU[5] and Mickaël HEDDE[8]

[1]*Normandie Univ, Université de Rouen Normandie (UNIROUEN), Centre National de la Recherche Scientifique (CNRS), M2C, Rouen 76000 (France)*

[2]*Institute of Earth Surface Dynamics (IDYST), Geopolis, University of Lausanne, Lausanne 1015 (Switzerland)*

[3]*Institut Français du Pétrole Energies Nouvelles (IFPEN), Earth Sciences and Environmental Technologies Division, Rueil-Malmaison 92852 (France)*

[4]*Institute of Earth Sciences (ISTE), Geopolis, University of Lausanne, Lausanne 1015 (Switzerland)*

[5]*Normandie Univ, Université de Rouen Normandie (UNIROUEN), Institut National de Recherche pour l'Agriculture, l'Alimentation et l'Environnement (INRAE), Laboratoire Étude et COmpréhension de la bioDIVersité (ECODIV), Rouen 76000 (France)*

[6]*Laboratory of Microbiology, Institute of Biology, University of Neuchâtel, Neuchâtel 2000 (Switzerland)*

[7]*Centre d'Ecologie Fonctionnelle et Evolutive (CEFE), Université de Montpellier, CNRS, Ecole Pratique des Hautes Etudes (EPHE), Institut de Recherche pour le Développement (IRD), Montpellier 34000 (France)*

[8]*Eco&Sols, INRAE, IRD, Université de Montpellier, Montpellier 34000 (France)*

ABSTRACT

Soil organic matter (SOM) is a complex heterogeneous mixture formed through decomposition and organo-mineral interactions, and characterization of its composition and biogeochemical stability is challenging. From this perspective, Rock-Eval® is a rapid and efficient thermal analytical method that combines the quantitative and qualitative information of SOM, including several parameters related to thermal stability. This approach has already been used to monitor changes in organic matter (OM) properties at the landscape, cropland, and soil profile scales. This study was aimed to assess the stability of SOM pools by characterizing the grain size fractions from forest litters and topsoils using Rock-Eval® thermal analysis. Litter (organic) and topsoil samples were collected from a beech forest in Normandy (France), whose management in the last 200 years has been documented. Fractionation by wet sieving was used to separate large debris ($>$ 2 000 μm) and coarse (200–2 000 μm) and fine particulate OM (POM) (50–200 μm) in the organic samples as well as coarse (200–2 000 μm), medium (50–200 μm), and fine ($<$ 50 μm) fractions of the topsoil samples. Rock-Eval® was able to provide thermal parameters sensitive enough to study fine-scale soil processes. In the organic layers, quantitative and qualitative changes were explained by the progressive decomposition of labile organic compounds from plant debris to the finest organic particles. Meanwhile, the grain size fractions of topsoils presented different characteristics. The coarse organo-mineral fractions showed higher C contents, albeit with a different composition, higher thermal stability, and greater decomposition degree than the plant debris forming the organic layer. These results are consistent with those of previous studies that microbial activity is more effective in this fraction. The finest fractions of topsoils showed low C contents, the highest thermal stability, and low decomposition degree, which can be explained by the stronger interactions with the mineral matrix. Therefore, it is suggested that the dynamics of OM in the different size fractions be interpreted in the light of a plant-microbe-soil continuum. Finally, three distinct thermostable C pools were highlighted through the grain size heterogeneity of SOM: free coarse OM (large debris and coarse and fine particles), weakly protected OM in (bio)aggregates (coarse fraction of topsoil), and stabilized OM in the fine fractions of topsoil, which resulted from the interactions within organo-mineral complexes. Therefore, Rock-Eval® thermal parameters can be used to empirically illustrate the conceptual models emphasizing the roles of drivers played by the gradual decomposition and protection of the most thermally labile organic constituents.

Key Words: aggregate, decomposition, litter, organo-mineral interaction, plant-microbe-soil continuum, soil organic matter, thermal analysis, topsoil

Citation: Sebag D, Verrecchia E P, Adatte T, Aubert M, Cailleau G, Decaëns T, Kowalewski I, Trap J, Bureau F, Hedde M. 2022. Size fractions of organic matter pools influence their stability: Application of the Rock-Eval® analysis to beech forest soils. *Pedosphere*. **32**(4): 565–575.

INTRODUCTION

Thermal analyses are commonly used to measure the thermal stability of soil organic matter (SOM). In addition to various compositional parameters, thermal stability is considered a proxy for biogeochemical stability, defined as the bioavailability (or bioaccessibility) of SOM to decomposition by microorganisms (Plante *et al*., 2009). There is ample literature on this topic, and the association between "analytical" thermal stability and "functional" biogeochemical stability is much debated among different research schools even today. Many studies have investigated thermograms as proxies for SOM stability (Plante *et al*., 2011; Peltre *et al*., 2013), but the thermal oxidation of SOM remains controversial. In particular, the accuracy of oxidative thermal analyses (*i.e*., combustion) has been subjected to strong criticism, as the current approaches poorly discriminate biological recalcitrance and are sensitive to carbon (C) content (Peltre

*Corresponding author. E-mail: david.sebag@ifp.fr.

et al., 2013; Schiedung *et al*., 2017). Nevertheless, according to Gregorich *et al*. (2015), the Rock-Eval® analytical process "is fundamentally different than other thermal degradation techniques in that it involves use of an inert atmosphere and rapid heating rates, and because it characterizes the reaction products from heating rather than properties of the bulk sample".

Some studies have calibrated the results obtained using Rock-Eval® with reference to those obtained using the conventional techniques (Carrie *et al*., 2012; Delarue *et al*., 2013; Hare *et al*., 2014). For instance, Albrecht *et al*. (2015) compared the Rock-Eval® parameters with direct data on structural and conformational characteristics obtained using ^{13}C-cross-polarization magic-angle spinning nuclear magnetic resonance (CPMAS-NMR) and concluded that the precision of Rock-Eval® results was good enough to identify thresholds of organic matter (OM) quality and thermal stability induced by changes in microbial communities. Gregorich *et al*. (2015) combined Rock-Eval® analysis with X-ray absorption near-edge structure (XANES) spectroscopy and demonstrated that the loss of SOM generally involves preferential degradation of hydrogen (H)-rich compounds. Similarly, using a combination of thermal analysis, differential scanning calorimetry, and evolved gas analysis, Barré *et al*. (2016) demonstrated that persistent SOM is thermally more stable and contains fewer H-rich compounds (low hydrogen index (HI)) than labile SOM. Finally, Soucémarianadin *et al*. (2018) showed that Rock-Eval® could precisely reproduce labile C pools in soils identified by biological or physical approaches (*i.e*., soil respiration test and isolation of particulate OM (POM) *via* physical fractionation).

Furthermore, some higher-scale studies focused on functional compartments, including the coarse (cPOM) and fine free POM (fPOM) as well as the mineral-associated OM (MAOM) fractions. The cPOM and fPOM fractions typically exhibit a low thermostability, corresponding to the most labile C pools, while the MAOM fraction exhibits a high thermostability, corresponding to the most stable C pool (Saenger *et al*., 2013, 2015; Gregorich *et al*., 2015). Previous studies have mainly emphasized the role of OM stability in soil C sequestration, as controlled by various environmental drivers, such as vegetation cover, land use, and climate. However, some studies have offered different perspectives. For instance, Sebag *et al*. (2016) illustrated the relevance of two combined thermal indices derived from the pyrolytic step of Rock-Eval® analysis to study the dynamics of a more reactive fraction of SOM—pyrolysable C. Indeed, these thermal indices are highly correlated when the stabilization processes are driven by the gradual decomposition of thermolabile fractions (Albrecht *et al*., 2015; Sebag *et al*., 2016; Matteodo *et al*., 2018; Thoumazeau *et al*., 2020). Such correlations are frequently observed in OM-rich samples and are interpreted to be a consequence of the progressive decomposition of POM (Lehmann and Kleber, 2015). In contrast, OM-poor samples and certain soil classes, such as Podzols or Arenosols, exhibit a deviation from these trends and instead present the interactions between the organic fraction and mineral matrix (Saenger *et al*., 2015; Sebag *et al*., 2016; Matteodo *et al*., 2018; Malou *et al*., 2020).

This body of knowledge supports the hypothesis that a decomposition (I) index-stability (R) index diagram integrates the intrinsic stability (or biological recalcitrance) of OM (*i.e*., the energy input to break down organic molecules) and the stabilization of SOM through interactions with soil minerals (*i.e*., the energy required to break the bonds between SOM and mineral particles). Here, we tested this hypothesis by characterizing the Rock-Eval® signatures (organic C content, composition, and thermal indices) of bulk samples as well as various size fractions of the organic (litter) and topsoil layers from a beech forest. More precisely, we monitored the evolution of the thermal status of these samples, representing a continuum from the most labile forms in the organic layers (biogenic precursors) to the most stable ones in the subsoil layers.

MATERIALS AND METHODS

Study site and previous studies

The study site, with an area of 7 200 ha, was located in the Eawy State Forest, Normandy, France (1°18′ E, 49°44′ N). Its management in the last 200 years has been documented. The climate is oceanic temperate, with a mean annual temperature of 10 °C and mean annual precipitation of 800 mm. The soil is an Endogleyic Dystric Luvisol (FAO, 2006), developed on a $>$ 80-cm-thick layer of loess (silty texture), overlying the clay-with-flint parent material. Soil texture was similar among stands, with 130 g kg^{-1} clay, 700 g kg^{-1} silt, and 170 g kg^{-1} sand. The understory vegetation is a characteristic *Endymio-Fagetum* type, according to phytosociological classification (Durin *et al*., 1967).

Research studies have been performed over the past 10 years on the soil biota (microorganisms, mesofauna, and macrofauna) (Aubert *et al*., 2003; Hedde *et al*., 2007; Chauvat *et al*., 2011; Trap *et al*., 2011c) and SOM dynamics (litter decomposition, nitrogen (N) cycling, and soil C stock) (Aubert *et al*., 2004, 2006, 2010; Hedde *et al*., 2008, 2010; Trap *et al*., 2011a, b) in this region. The key findings of these studies are summarized in a review by Aubert *et al*. (2018). Over a 200-year chronosequence, it has been shown that the best performance of the forest ecosystem, defined as high OM recycling, was achieved when the plant and soil communities jointly exhibited limited similarities and complementarities in species functional traits. Although soil and humus C fractions have been studied in terms of mass, content, and stock dynamics, their stability warrants further assessment.

Sampling

The studied sample set (Table I) originates from previous studies on SOM dynamics (*i.e.*, quantitative and qualitative changes) and combines morphological description, physical fractionation, and C and N determinations (Hedde *et al.*, 2008). The selected plots cover the entire silvicultural cycle (over a period of 200 years). Plots have always been occupied by the same tree species (*Fagus sylvatica* L.), minimizing possible changes in the chemical composition of plant debris.

A total of 75 humipedons, *i.e.*, the upper parts of soil constituted by organic and/or organo-mineral horizons (Zanella *et al.*, 2018), were described for 15 stands, with five points per stand within a 25 cm × 25 cm quadrat. Each humipedon was separated into the OL, OF/OH, and A horizons according to their macroscopic morphological characteristics (Jabiol *et al.*, 2007). This horizon nomenclature corresponds to the United States Department of Agriculture (USDA) nomenclature as follows: OL = Oi, OF = Oe, and OH = Oa. Thereafter, samples were collected from the horizons in delimited areas, stored in plastic bags, air-dried, and weighed.

Fractionation

Physical fractionation was performed on the samples of OF/OH horizons and topsoils using a method that depends on the nature of the samples (Hedde *et al.*, 2008).

We assumed that the state of decomposition of POM in the organic layers is a function of its particle size, as decay induces fragmentation. In the OF/OH samples, logs, herbaceous vegetation litter, and beech fruits (masts and nuts) were separated from the remaining OM (rOM) and weighed. Then, the size distribution of the rOM was assessed by wet sieving using a vibratory sieve shaker. The rOM was moistened with deionized water, deposited on the top sieve, and passed through 2 000-, 200-, and 50-μm meshes. The obtained fractions were subjected to flotation and panning in water to separate the light fraction, comprising light OM, from the heavy fraction, mainly comprising mineral material. The fractions were oven-dried (40 °C for 48 h) and weighed. The finest mineral fraction (< 50 μm) was excluded. The resulting light organic fractions (O-fractions) included decaying beech leaves (large debris, > 2 000 μm), cPOM (O-coarse, 200–2 000 μm), and fPOM (O-medium, 50–200 μm). The O-coarse and O-medium fractions are comparable to the functional litter compartments O-cPOM and O-fPOM, respectively.

Furthermore, subsamples of air-dried topsoil (bulk A) were subject to physical dispersion of particles prior to fractionation, as described by Balesdent *et al.* (1991). The soil samples were shaken with glass beads on an end-over-end shaker for 16 h. The dispersed fractions were then separated at 2 000, 200, and 50 μm through wet sieving. The coarsest fraction (> 2 000 μm) was very limited in the studied soils, as they developed from loess parent material. Therefore, this fraction was removed. In the remaining fractions, light POM was separated from the heavy minerals by flotation and sedimentation in water. The < 50 μm suspension was flocculated with $CaCl_2$. All fractions were oven-dried and weighed. The obtained organo-mineral fractions (A-fractions) were as follows: A-coarse fraction (200–2 000 μm), A-medium fraction (50–200 μm), and A-fine fraction (< 50 μm). These A-fractions do not exactly match the functional soil compartments conventionally referred to as cPOM, fPOM, occluded POM (oPOM), and MAOM. Nevertheless, examinations under a binocular microscope confirmed that the A-coarse fraction was mostly composed of POM, whereas the A-fine fraction was extremely poor in it. Consequently, we assumed it reasonable to consider the A-coarse and A-fine fractions to be relatively enriched with POM and MAOM, respectively, with the A-medium fraction as a composite fraction.

TABLE I

Statistics (1st quartile, median, and 3rd quartile) of the measured or calculated values of Rock-Eval® parameters[a)] for litters (O horizon) and topsoils (A horizon) and their respective size fractions of the soil sample set for the study site in the Eawy State Forest, Normandy, France

Sample	TOC	TpS2	HI	OI	*I* index	*R* index
	g kg^{-1}	°C	mg HC[b)] g^{-1} TOC	mg CO_2 g^{-1} TOC		
All samples	97, 412, 502	372, 418, 458	276, 315, 394	77, 118, 188	0.13, 0.21, 0.39	0.42, 0.52, 0.57
Litter						
Bulk sample	478, 487, 506	369, 371, 372	270, 287, 297	115, 119, 121	0.48, 0.49, 0.51	0.35, 0.36, 0.37
Large debris (> 2 000 μm)	444, 498, 536	370, 372, 375	249, 264, 273	111, 120, 159	0.36, 0.39, 0.42	0.40, 0.42, 0.44
O-coarse (200–2 000 μm)	417, 501, 506	373, 374, 375	249, 267, 295	100, 111, 197	0.31, 0.34, 0.39	0.42, 0.46, 0.49
O-medium (50–200 μm)	346, 423, 489	366, 371, 373	294, 342, 378	69, 77, 236	0.35, 0.35, 0.36	0.43, 0.45, 0.46
Topsoil						
Bulk sample	38, 46, 57	461, 463, 464	299, 312, 319	143, 144, 153	0.15, 0.17, 0.19	0.54, 0.55, 0.57
A-coarse (200–2 000 μm)	382, 486, 584	426, 432, 433	349, 382, 410	41, 50, 268	0.07, 0.09, 0.10	0.55, 0.57, 0.58
A-medium (50–200 μm)	190, 244, 268	427, 437, 451	315, 370, 394	50, 63, 212	0.12, 0.15, 0.17	0.55, 0.57, 0.59
A-fine (< 50 μm)	25, 32, 58	463, 464, 465	316, 338, 366	97, 151, 292	0.11, 0.12, 0.15	0.59, 0.60, 0.62

[a)] TOC = total organic carbon; TpS2 = maximum cracking temperature; HI = hydrogen index; OI = oxygen indexl; *I* index = decomposition index; *R* index = stability index.
[b)] Hydrocarbon.

Rock-Eval® thermal analysis

Analyses were performed using 30–70 mg of powdered samples with Rock-Eval® 6 (Vinci Technologies, France). All analytical processes and protocols followed in the present study are described elsewhere (Lafargue *et al.*, 1998; Behar *et al.*, 2001; Disnar *et al.*, 2003; Sebag *et al.*, 2016). The Rock-Eval® analysis is based on continuous measurement of gas effluents, *i.e.*, hydrocarbon (HC), carbon oxide (CO), and carbon dioxide (CO_2), released during the thermal cracking of organic compounds (and thermal decomposition of carbonate minerals) under pyrolytic conditions (from 200 to 650 °C at 25 °C min^{-1} in an inert atmosphere), followed by the combustion of residual C (from 300 to 850 °C in an oxidative atmosphere). The resulting thermograms were used to calculate the standard parameters by integrating the amounts of HC, CO, and CO_2 within the defined temperature limits (Lafargue *et al.*, 1998; Behar *et al.*, 2001).

Over the past 15 years, applications in environmental sciences have allowed the measurement of OM quality changes in soils and recent sediments as well as the quantification of C fluxes and stocks in various environments. In general, these analyses are based on the four standard parameters of total organic C (TOC), maximum cracking temperature (TpS2), HI, and oxygen index (OI). The parameter TOC is calculated as the sum of all C effluents (*i.e.*, HC, CO, and CO_2). In soil samples, TOC represents the amount of organic C and has been well calibrated in previous studies (Disnar *et al.*, 2003; Saenger *et al.*, 2013; Malou *et al.*, 2020). The TpS2 corresponds to the oven temperature at which the maximum HC is released during pyrolysis. The HI corresponds to the amount of HC released during pyrolysis relative to TOC. In soil samples, decrease in HI along soil profiles is related to the dehydrogenation of organic compounds during pedogenesis (Disnar *et al.*, 2003; Barré *et al.*, 2016). The OI corresponds to the amount of carbon dioxide (CO_2) released during pyrolysis before reaching the temperature of 400 °C for CO and 500 °C for CO_2 (*i.e.*, from the cracking of organic compounds, not from the thermal decomposition of carbonates), expressed relative to TOC. In soil samples, increase in OI along soil profiles is related to relative oxygenation, which is often interpreted as the aromatization of organic compounds.

In addition to the above standard parameters, Disnar *et al.* (2003) have proposed using the shape of thermograms to obtain additional information about SOM quality. In the present study, we used the R index to measure the contribution of thermoresistant and thermorefractory C pools and the I index to quantify the preservation of the thermolabile C pool (Sebag *et al.*, 2016). Both indices are derived from the integrated S2 areas between specific bounds (200–400, 400–460, and > 460 °C), usually interpreted as specific thresholds of the thermal stability of organic compounds, separating the thermolabile, thermoresistant, and thermorefractory C pools (Figs. S1 and S2, see Supplementary Material for Figs. S1 and S2) (Disnar *et al.*, 2003; Sebag *et al.*, 2006; Saenger *et al.*, 2013, 2015). In addition, both indices are calculated from S2 thermograms (*i.e.*, HC released by thermal cracking under pyrolytic conditions), which are little or not sensitive to the interference of mineral matrix and catalytic reactions. These indices have been developed to study the most reactive fraction of SOM (*i.e.*, richer in H bonds and thermolabile), which is directly involved in short-term changes in soil C dynamics. Nevertheless, as recommended by Schiedung *et al.* (2017), these thermal indices do not consider the various labile pools, that is, they do not reflect biological stability, but focus on SOM biogeochemical stability.

RESULTS

Standard Rock-Eval® parameters

As shown in Table I, TOC varied among the bulk samples (420–550 g kg^{-1} in litters and 30–80 g kg^{-1} in topsoils), O-fractions (> 410 g kg^{-1} in large debris, 340–560 g kg^{-1} in O-coarse, and 210–600 g kg^{-1} in O-medium), and A-fractions (380–740 g kg^{-1} in A-coarse, 190–400 g kg^{-1} in A-medium, and 15–60 g kg^{-1} in A-fine). The boxplots show a fairly continuous decreasing trend from the OL horizon (only beech litter) and large debris toward the O-fractions and A-coarse fraction and a drastic decreasing shift toward the A-medium and A-fine fractions (Fig. 1).

The TpS2 exhibited a typical pattern, with low values (*ca.* 370 °C) for the litters and their size fractions and high

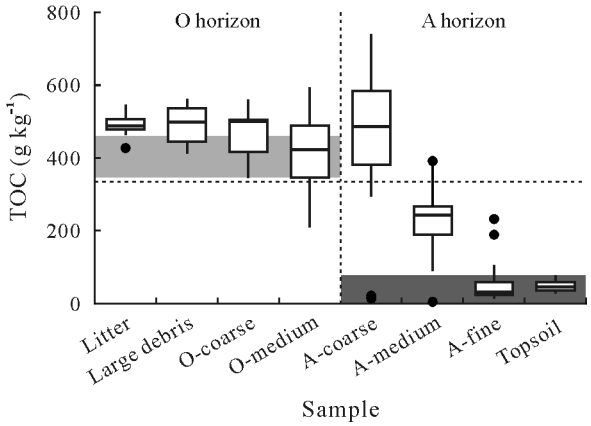

Fig. 1 Boxplots of soil total organic carbon (TOC) contents of litters (O horizon) and topsoils (A horizon) and their respective size fractions of the soil sample set for the study site in the Eawy State Forest, Normandy, France. The horizontal bands indicate the range of values for the bulk samples of litters (gray) and topsoils (dark gray) from the dataset of Sebag *et al.* (2016). Boxes show 25–75 percentiles, vertical lines show 10–90 percentiles, horizontal lines within boxes are median values ($n = 25$), and points outside the boxes represent outliers. Large debris > 2 000 μm; O-coarse = 200–2 000 μm; O-medium = 50–200 μm; A-coarse = 200–2 000 μm; A-medium = 50–200 μm; A-fine < 50 μm. The dash line indicates the mean of all samples.

values (420–470 °C) for topsoils and their size fractions (Fig. 2).

The HI showed great variability among samples (Fig. 2). Specifically, litter, large debris, and O-coarse presented low HI variability with a range of 225–330 mg HC g^{-1} TOC and a mean of 275 mg HC g^{-1} TOC, whereas O-medium presented high HI variability with a range of 240–420 mg HC g^{-1} TOC and a mean of 340 mg HC g^{-1} TOC. Moreover, the HI values and their dispersion were markedly greater in all A-fractions (290–900 mg HC g^{-1} TOC), but the values decreased from the A-coarse (610 mg HC g^{-1} TOC) to A-medium (555 mg HC g^{-1} TOC) and A-fine (455 mg HC g^{-1} TOC). The HI values of the bulk topsoil samples (255–330 mg HC g^{-1} TOC) were quite close to those of O-coarse.

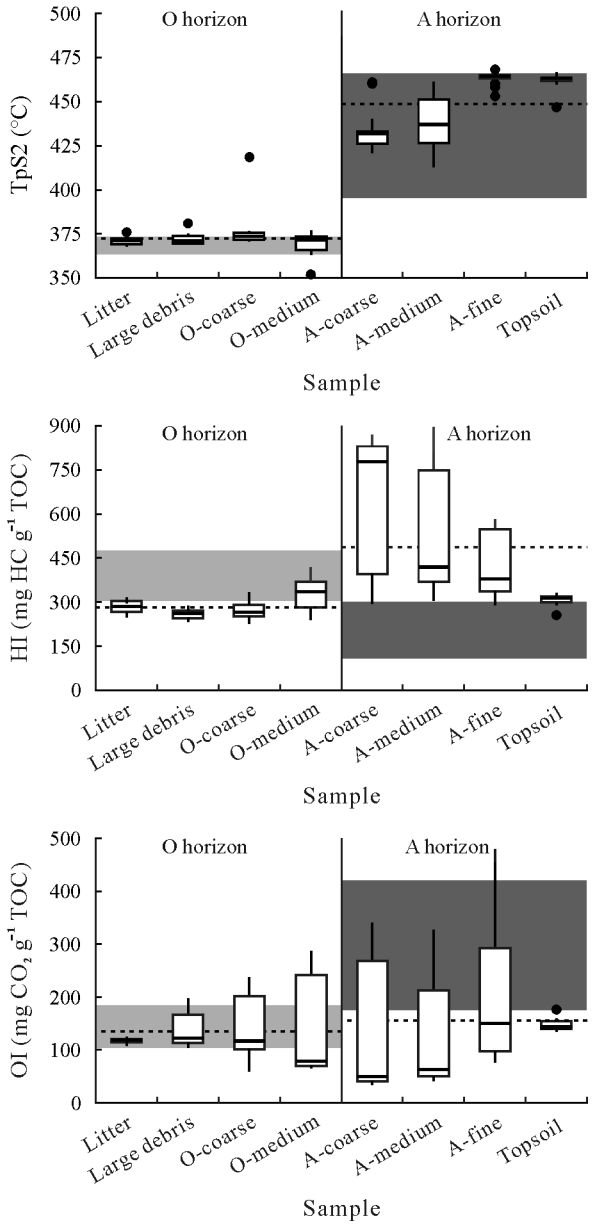

Fig. 2 Boxplots of standard Rock-Eval® parameters for litters (O horizon) and topsoils (A horizon) and their respective size fractions of the soil sample set for the study site in the Eawy State Forest, Normandy, France. TpS2 = maximum cracking temperature; HI = hydrogen index; OI = oxygen index; HC = hydrocarbon; TOC = total organic carbon. Boxes show 25–75 percentiles, vertical lines show 10–90 percentiles, horizontal lines within boxes are median values ($n = 25$), and points outside the boxes represent outliers. Large debris > 2 000 µm; O-coarse = 200–2 000 µm; O-medium = 50–200 µm; A-coarse = 200–2 000 µm; A-medium = 50–200 µm; A-fine < 50 µm. The horizontal bands indicate the range of values for the bulk samples of litters (gray) and topsoils (dark gray) from the dataset of Sebag *et al*. (2016). The left and right dash lines indicate the means of all samples of litters and topsoils, respectively.

The OI patterns differed according to the horizons (Fig. 2). The OI distribution was particularly remarkable in the O-fractions. In each fraction, the majority of samples showed a low OI, ranging from 75 to 150 mg CO_2 g^{-1} TOC (median ≈ 120 mg CO_2 g^{-1} TOC). However, the OI dispersion increased with decreasing fraction size, ranging from 75 to 250 mg CO_2 g^{-1} TOC in O-medium. Meanwhile, the OI values and their dispersion increased from A-coarse (*ca*. 35–340 mg CO_2 g^{-1} TOC) to A-fine (75–480 mg CO_2 g^{-1} TOC), but decreased for the bulk topsoil samples (135–175 mg CO_2 g^{-1} TOC).

I-R index diagram

The I-R index diagram (Fig. 3a) presented a drastic contrast and a large hiatus between the litters (I index > 0.9, R index < 0.4) and topsoils (I index < 0.5, R index > 0.5), with the O-fractions distributed along the regression line, hereafter referred as the "decomposition line" as identified by Sebag *et al*. (2016). The A-fractions were distributed around the topsoil samples. The A-medium fractions were distributed along the decomposition line, the A-fine fractions were distributed above it, and the A-coarse fractions were distributed below it. The R index ranges of the A-coarse and A-medium fractions were close (Fig. 3b), highlighting the relatively low I index values of coarse organic constituents (> 200 µm). Conversely, the I index ranges of the A-fine and A-medium fractions were close (Fig. 3c), highlighting the relatively high R index values of fine organic constituents (< 50 µm).

DISCUSSION

Rock-Eval® parameters and SOM composition

The standard Rock-Eval® parameters (*i.e*., TOC, TpS2, HI, and OI) represent the general trends and signatures (Figs. 1 and 2, Table I) related to the decomposition of SOM and changes in its chemical composition. The present results are consistent with the findings of previous studies using Rock-Eval® (Di-Giovanni *et al*., 1998; Disnar *et al*., 2003; Sebag *et al*., 2006, 2016; Saenger *et al*., 2013).

The TOC content (Fig. 1) decreased gradually from the large debris to A-medium fractions and drastically in the

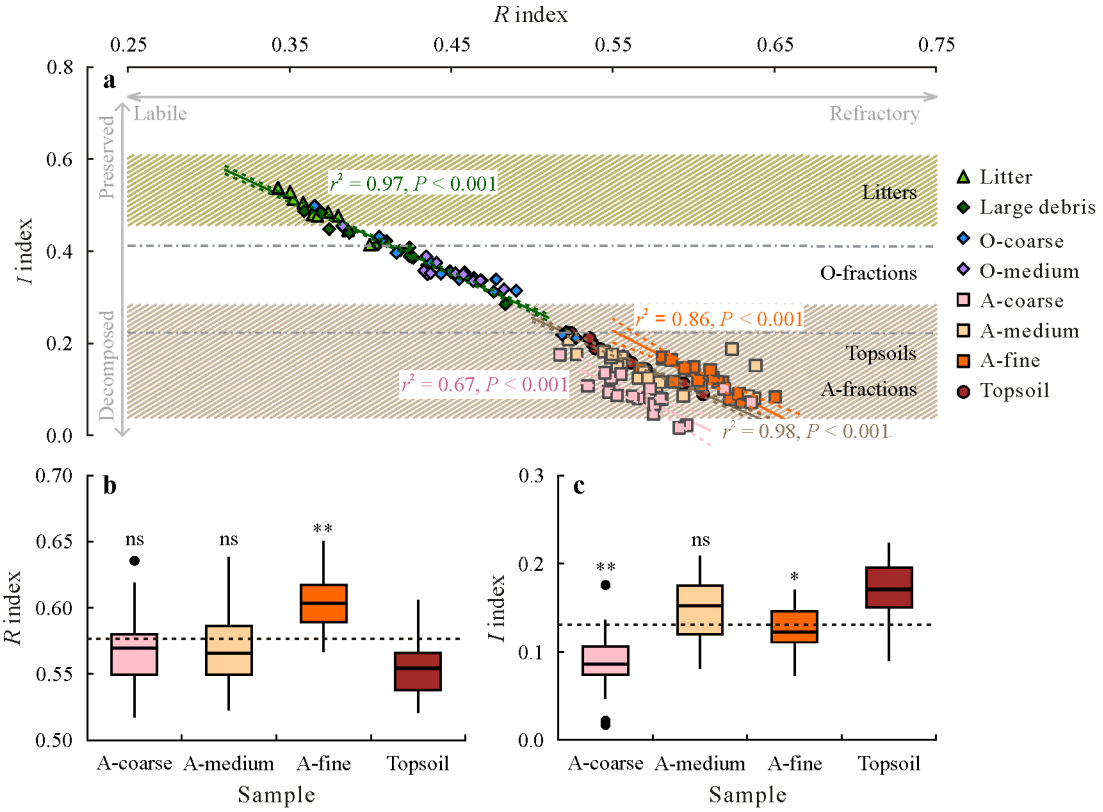

Fig. 3 Diagram (a) and boxplots (b and c) showing the relationship between decomposition (I) index and thermal stability (R) index of litters (O horizon) and topsoils (A horizon) and their respective size fractions of the soil sample set for the study site in the Eawy State Forest, Normandy. The dash-dotted lines indicate the empirical limits between litters, O-fractions, and topsoils. The horizontal bands indicate the ranges of values for the bulk samples of litters (light green) and topsoils (light brown) from the dataset of Sebag *et al.* (2016). The central regression line represents the "decomposition line" calculated using the dataset of Sebag *et al.* (2016), and the dotted lines on both sides indicate the 95% confidence interval. The other two regression lines correspond to the A-coarse fraction (bottom) and the A-fine fraction (upper). Boxes show 25–75 percentiles, vertical lines show 10–90 percentiles, horizontal lines within boxes are median values ($n = 25$), and points outside the boxes represent outliers. A-coarse = 200–2 000 µm; A-medium = 50–200 µm; A-fine < 50 µm. The R and I indices of A-fractions were compared with those of the topsoils, with * indicating significant difference at $P < 0.05$, ** indicating significant difference at $P < 0.01$, and ns indicating no significant difference ($P > 0.05$). The dash lines indicate the means of all samples.

A-fine fractions. Hedde *et al.* (2008) have already underlined this trend in their studied soils and reported that these changes can be explained by the loss of C-based compounds through leaching or microbial decay. Consequently, in topsoils, this trend reflects the increasing proportion of the mineral matrix with decreasing grain size of the fractions (up to 80% in the finest A-fine fraction). These quantitative results (*i.e.*, C content) confirm that the fractionation protocol (*i.e.*, sieving and flotation in water) separated the coarse fraction (A-coarse) enriched in OM from the fine fraction (A-fine) enriched in minerals. In addition, relative contributions indicated the predominance of certain fractions in the samples. Specifically, the organic layers were mainly composed of large debris (> 2 mm; 60%–70% of C mass), while the topsoils were mainly composed of A-fine (32%–45% of C mass) (recalculated from Hedde *et al.*, 2008).

Furthermore, based on TpS2, HI, and OI, the litters presented a typical homogeneous signature of fresh plant tissues, with all values falling within the ranges reported by Sebag *et al.* (2016) (TpS2 ≈ 370 °C, HI ≈ 250–300 mg HC g^{-1} TOC, and OI ≈ 120 mg CO_2 g^{-1} TOC), which also characterizes the OF/OH fractions (large debris and O-coarse). Compared with fresh plant remains reported by previous works, the signatures (*i.e.*, OM quality) of litters, large debris and O-coarse, reflect a low decomposition, with no real impact on the bulk composition of biogenic inputs (*i.e.*, plant tissues).

Similar to litters, the topsoils presented TpS2, HI, and OI values within the previously reported ranges (Sebag *et al.*, 2016) (TpS2 ≈ 440–460 °C, HI ≈ 260–400 mg HC g^{-1} TOC, and OI ≈ 150–250 mg CO_2 g^{-1} TOC). Meanwhile, unlike the homogeneous O-fractions, the A-fractions exhibited diverse signatures. The stepwise increase in TpS2 reflects increase in thermal stability with decrease in grain size. This trend, related to decrease in HI and increase in OI, can be interpreted as a consequence of decomposition, along with other processes occurring in the superficial organic layers. However, very high HI and very low OI of the A-coarse fraction indicate a drastic change in the composition of this fraction compared with that of the O-fractions. Such a change

may be related to microbial OM, whose biogenic precursors are H-rich and O-poor. These conclusions are corroborated by the patterns of the C/N ratios. In the same samples, Hedde *et al*. (2008) found the maximum C/N ratio (*ca*. 27) in the litters, with the values gradually decreasing with decreasing size of the O-fractions (23–24, 19–20, and 16–18 for large debris, O-coarse, and O-medium, respectively). However, the ratio in the A-coarse fraction was 20–22, between those reported for large debris and O-coarse.

From this perspective, the fractionation protocol (*i.e*., sieving and flotation in water) may have separated the following fractions: i) homogenous O-fractions, comprising coarse and fine free OM corresponding to fragmented but weakly decomposed (high HI and low TpS2) plant debris (*i.e*., primary production), ii) an A-coarse fraction enriched in weakly decomposed (very high HI) microbial OM (*i.e*., secondary production), iii) an A-fine fraction enriched in soil minerals and stabilized OM (high TpS2), and iv) an A-medium fraction, intermediate between the coarse and fine A-fractions, confirming its composite nature. Finally, these results illustrate the concept of the plant-microbe-soil continuum. However, for comparison between the organic and topsoil fractions, the compositional indices (HI and OI) appear, on the one hand, insufficiently sensitive to measure the progressive decomposition of plant debris in the litter, and on the other, too sensitive to the compositional changes. It is, therefore, difficult to distinguish between the various processes (*i.e*., biogenic precursor composition, labile pool decomposition, and organo-mineral interactions) that may explain the changes in thermal stability measured by TpS2.

Thermal stability and gradual decomposition

The I-R index diagram (Fig. 3) shows the patterns of SOM quality (I index) and thermal stability (R index) as a function of the grain size fractions. In a previous study, high continuous input of OM was observed in all stands based on the measurement of litter production (Trap *et al*., 2011a). As expected, the litters (low decomposition and low stability) differ drastically from topsoils (high decomposition and high stability). The hiatus between litters and topsoils was also evident between the O- and A-fractions, reflecting a major threshold. Considering that thermal stability can integrate several mechanisms of OM stabilization (Saenger *et al*., 2013; Gregorich *et al*., 2015; Sebag *et al*., 2016), we assume that this gap is related to multiple interactions between the organic fractions and mineral matrix.

The large debris, O-coarse, and O-medium are derived directly from the aerial litters which first enter the soil through accumulation in the OL horizon. However, they displayed increasing decomposition (*i.e*., I index values) and thermal stability (*i.e*., R index values). First, both indices of the bulk litter and O-fractions were strongly correlated, indicating that the gradual decomposition of labile pools (decrease in I index) is a major driver of OM stabilization (increase in R index) (Albrecht *et al*., 2015; Matteodo *et al*., 2018; Thoumazeau *et al*., 2020). Second, the O-fractions overlapped with one another, indicating that their evolution (*i.e*., gradual decomposition of labile pools) is probably fairly continuous and comparable. Third, the variances of both indices were large for all O-fractions, which can be explained by the different ages of the studied plots. Indeed, the large debris and O-coarse fractions showed low variability for each stand but high variability during the sylvicultural cycle (Trap *et al*., 2011a). In contrast, the O-medium fractions appeared relatively stable along the 200-year chronosequence. These results extend the conclusions of previous studies using the same sample set, which showed that the modification in soil biota activity may be responsible for changes in the decaying processes and SOM dynamics (Hedde *et al*., 2008; Trap *et al*., 2013). Thermal analysis shows that the stability of the coarser fractions in organic layers (large debris and O-coarse) could be affected by temporal changes in soil biota activity (Trap *et al*., 2011c), whereas the stability of the finer fractions (O-medium) varies slightly over time. In the present study, topsoil and A-medium fractions were plotted along the decomposition line (Fig. 3), indicating that the gradual decomposition of the most labile compounds continues to play a major role in the stabilization of SOM. Conversely, the A-coarse and A-fine fractions were plotted below and above the decomposition line, respectively, indicating differences in the processes of stabilization. The ranges of R index were comparable between the A-coarse and A-medium fractions, indicating that the stability benefit (positive R shift compared with the O-fraction) was of the same order of magnitude for both fractions and may be related to the physical protection provided by the mineral matrix to all A-fractions. Nevertheless, the lower I index values of A-coarse reflect a higher decomposition of thermolabile constituents. This may be explained by the differences in aggregate sizes for each fraction, as occlusion is more efficient in micro- than in macro-aggregates (Six *et al*., 2002). However, the structural analysis of these soils has demonstrated that they are primarily composed of micro-aggregates (Trap *et al*., 2011a). Therefore, another explanation would be the relationship between thermal status and compositional indices: an advanced decomposition of the most labile fraction (low I index) coincides with a significant increase in HI. However, this relationship is contrary to the evolution of plant debris in litters and soils (*i.e*. decrease in HI). The microbial activity may provide interesting clues: I index values can be influenced by intense microbial decomposition of plant OM, whereas HI values reflect the synthesis of H-rich microbial OM.

Finally, the A-fine fraction presented a higher thermal stability (highest R index) than the A-medium fraction, albeit

without differences in the decomposition of the thermolabile pool (I index). This may be explained by the strong interactions between this finest OM fraction and the mineral matrix: both A-medium and A-fine fractions would be physically protected in micro-aggregates, but the latter would also be protected at an even finer scale (occlusion within clay microstructures, adsorption on mineral surfaces, and/or formation of organo-mineral complexes).

From this perspective, the I-R index diagram emphasizes that the thermal stability (R index) of topsoil OM changes continuously due to the gradual decomposition (I index) of the most labile pools (*i.e*., a strong inverse correlation between the two indices along the decomposition line). In addition, different thermal statuses can be assigned depending on the type of interaction with the mineral matrix. The organic particles constituting the A-coarse fraction (200–2 000 μm) are larger than the topsoil micro-aggregates. Therefore, they are poorly protected by occlusion and more easily accessible and decomposed by soil microorganisms. The organic particles forming the A-medium fraction (50–200 μm) are better protected in micro-aggregates (occlusion) and less bioavailable for soil microorganisms. However, because of the separation protocol, we cannot rule out the possibility of the presence of a composite A-medium fraction with an intermediate signature between the two functional compartments (POM and MAOM). The organic constituents of the A-fine fraction (< 50 μm) are diluted in an abundant mineral matrix. As the A-fine fraction had a higher thermal stability without showing a further decomposition state compared with the A-medium fraction, it is reasonable to assume that this is related to the additional protection provided by the mineral matrix (*i.e*., occlusion in clay microstructures, adsorption, and/or complexation).

Finally, the main conclusions of this study are summarized in Table II, which shows the relationships between the thermal stability indices, size fractions, thermal C pools (labile, resistant, and refractory), and some pedogenic processes. The differential mineralization in organic fractions causes the decrease of labile C pool with a proportional increase in the resistant and refractory pools, ultimately resulting in the decrease of the decomposition index (I index calculated as labile/resistant ratio) and the relative increase of stability (R index calculated as resistant + refractory). As the changes in resistant and refractory C pools directly result from the decrease in the labile C pool, this free OM is plotted on the decomposition line. Conversely, all A fractions are stabilized through processes related to matrix protection. These mechanisms attenuate decomposition, and the protected pools, even the labile one, are stabilized. Consequently, the labile C pool decreases in the favor of the resistant C pool, resulting in proportional shifts in decomposition (lower I index) and stability (higher R index). The same mechanisms allow the discrimination of the fraction occluded in micro-aggregates (on the decomposition line) and the one weakly protected (below the decomposition line). Likewise, interactions with the soil mineral fraction provide protection strong enough to increase the resistant and refractory pools, thus increasing stability (above the decomposition line).

SOC stability and SOM dynamics

We consider that changes in OM quality (I index, HI, and OI) and thermal stability (R index and TpS2) reflect

TABLE II

Relationships between litter (O horizon) and topsoil (A horizon) organic matter (OM) thermal stability indices, size fractions, thermal C pools, and some pedogenic processes

Sample[a)]	Characteristic	Stabilization process	C pool[b)]			I index[c)]	R index[d)]	Position[e)]
			L	Rs	Rf			
Litter	Labile OM mineralization	Resistant OM preservation	Decrease	Increase	Increase	Small decrease	Small increase	On
Topsoil	Incorporation in mineral matrix	Physical protection	Decrease	Increase		Small decrease	Small increase	On
A-coarse	Weekly protected, labile OM mineralization, incorporation in mineral matrix	Resistant OM preservation, physical protection	Decrease	Increase	Increase	Large decrease	Moderate increase	Below
A-medium	Well-protected, labile OM mineralization, incorporation in mineral matrix, long-time evolution	Resistant OM preservation, physical protection, occlusion (micro-aggregates)	Decrease	Increase		Moderate decrease	Moderate increase	On
A-fine	Stabilized, labile OM mineralization, incorporation in mineral matrix, very long-time evolution	Resistant OM preservation, physical protection, occlusion (micro-aggregates), adsorption (mineral)	Decrease	Increase	Increase	Moderate decrease	Large increase	Above

[a)] A-coarse = 200–2 000 μm; A-medium = 50–200 μm; A-fine < 50 μm.
[b)] L = thermolabile; Rs = thermoresistant; Rf = thermorefractory.
[c)] Decomposition index, calculated as L/Rs.
[d)] Stability index, calculated as Rs + Rf.
[e)] On = on the decomposition line; Below = below the decomposition line; Above = above the decomposition line.

the consequences of differences in the biogeochemical stability of grain size fractions. Indeed, our results illustrate a conventional model of biogeochemical stabilization, that is, splitting OM into free and protected pools, the latter being protected in organo-mineral assemblages, (bio)aggregates, and/or clay microstructures (von Lützow *et al*., 2007). It is straightforward to relate this conventional pool model with the interpretation of the I-R index diagram. Indeed, the gap in the decomposition degree (I index) can be seen as a distinction between the free POM in litters, large debris, O-coarse, and O-medium and the protected OM, including the weakly protected A-coarse, well-protected A-medium, and strongly stabilized A-fine, according to their relative positions in the I-R index diagram (Fig. 3). In the litters, the different fractions are, by nature, enriched in free POM and are probably rapidly turned over. In topsoils, any discussion about residence times remains speculative, as the separation protocol does not isolate pure functional compartments.

However, OM dynamics can be represented schematically by crossing the quantitative (C stocks) and qualitative (bulk composition and thermal stability) variables. Because the studied soils are comparable, the parameter TOC can be used to represent the relative changes in SOC content in various grain size fractions (Fig. 4). In the O horizon (*i.e*., litter and OF/OH horizons), OM changes are mainly related to biochemical processes (*i.e*., progressive decomposition and mineralization of labile compounds) driven by certain intrinsic OM properties, such as the structural stability of organic compounds, and extrinsic environmental factors, such as primary production, edaphic conditions, and biota. In the topsoils, the differences observed between various size fractions appear independent of the properties of the overlying organic layers but are directly related to their interactions with the mineral matrix (soil structure, mineral surfaces, and so on).

Thus, our results can be interpreted within the framework of the emergent view and current debate on SOC dynamics. As assumed by the conceptual model proposed by Schmidt *et al*. (2011), the Rock-Eval® analysis can clearly differentiate the organic and mineral samples (litter/topsoil and organic/mineral fractions) in terms of the OM content, composition, and thermal stability. In addition, changes in compositional parameters (HI and OI) appear to pinpoint the main stages of the plant-microbe-soil continuum by highlighting i) the source (*i.e*., plant remains) of organic particles in the organic layers, ii) the probable impact of organisms on the poorly protected topsoil coarse fractions, and iii) the specific signature of the fine fraction that dominates in topsoils. Moreover, the thermal parameters provide an empirical illustration of the soil continuum model developed by Lehmann and Kleber (2015). Indeed, the I-R index diagram graphically represents i) the progressive decomposition of the most labile compounds (*i.e*., decomposition line), which starts in the litter and continues down to the finest fraction of the topsoils, and ii) the clustering of the topsoil fractions related to the types of interactions between organic particles and soil minerals. At this point, the diagram also features the bioenergetic framework proposed by Williams and Plante

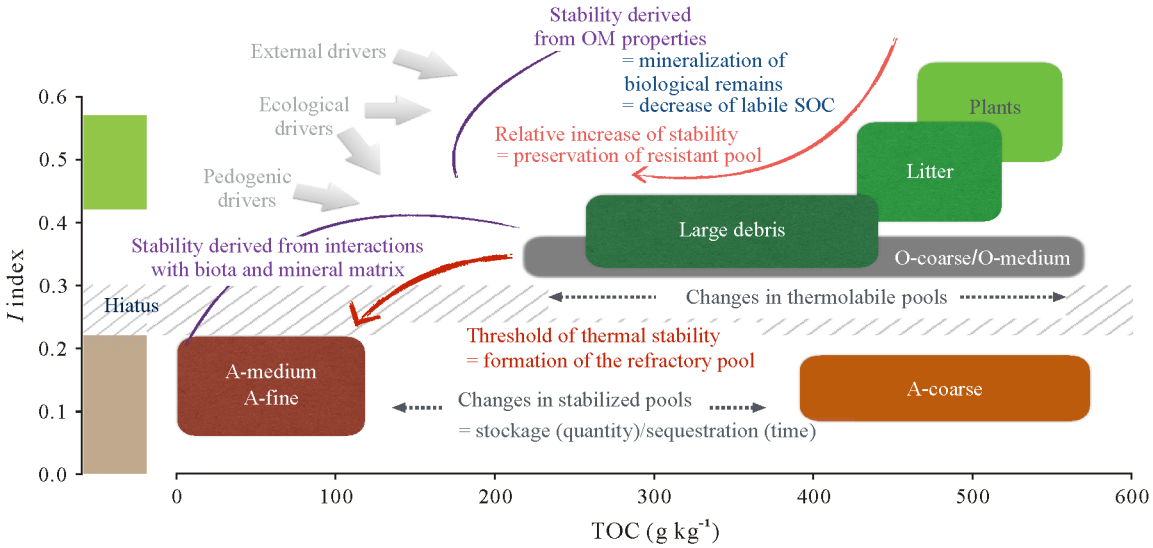

Fig. 4 Schematic showing that in litters (O horizon) and their size fractions (*i.e*., large debris, O-coarse, and O-medium), the mineralization of biological remains (decrease in TOC) increases SOM stability (decrease in I index) due to the preservation of the thermoresistant pool and in the various size fractions of the topsoils (A horizon) (*i.e*., A-coarse, A-medium, and A-fine), the interactions between biota and the mineral matrix increase SOM stability (decrease in I index) due to the formation of the thermorefractory pool. The increase in SOM stability leads to C sequestration. TOC = total organic carbon; SOM = soil organic matter; I index = decomposition index; large debris > 2 000 µm; O-coarse = 200–2 000 µm; O-medium = 5–200 µm; A-coarse = 200–2 000 µm; A-medium = 50–200 µm; A-fine < 50 µm. The boxes indicate the ranges of values for the bulk samples of litters (green) and topsoils (brown) from the dataset of Sebag *et al*. (2016).

(2018), which utilizes thermally determined activation energy and energy density to assess the persistence of SOM. Nevertheless, further studies are warranted to verify whether thermal pools can be assimilated into functional compartments and whether the R and I indices can be related to activation energy and energy density, respectively.

CONCLUSIONS

This study highlights some assets of the Rock-Eval® thermal analysis and its derived parameters to quantify the decomposition and stability of SOM. Various parameters, including HI, I index, and R index, which are related to the most reactive part of SOM, reflect changes in OM composition and thermal stability induced by decomposition of labile compounds as well as organo-mineral interactions in topsoils. Moreover, the combination of compositional and thermal indices assumes that at least three thermal C pools can be identified to model the grain size heterogeneity of SOM: i) free particulate plant-derived OM (low decomposition and low stability) in litters and their size fractions, ii) coarse weakly protected OM (high decomposition and high stability) probably partly decomposed by microorganisms in the organic fractions of topsoils, and iii) fine stabilized OM (high decomposition and high stability) related to the mineral fractions of topsoils. Although the thermal pools do not correspond exactly to the conventional functional compartments, they allowed us to elucidate the dynamics of OM in forest soils developed from loess in northwestern France. This case study accurately illustrates the concept of the plant-microbe-soil continuum and new emerging paradigms, contributing to a comprehensive understanding of OM formation and its fate in soil. Our findings underscore that the size and stoichiometry of the decomposition products and their interactions with the soil matrix determine their thermal stability. Further studies should focus on the evolution of the thermal properties of OM according to changes in soil (micro)biota over time.

ACKNOWLEDGEMENTS

Rock-Eval® is a trademark registered by the Institut Français du Pétrole Energies Nouvelles (IFPEN), France. Jean Trap's research was funded by the French "Ministère de l'Agriculture et de la Pêche", the "GIP ECOFOR" (No. 82005.20), and the "GRR-SER" (Environmental Sciences, Analysis and Risk Management). Mickaël Hedde's research was supported by the Haute-Normandie Region (France) in the framework of the GRR-SER and by the FR CNRS 3730 SCALE (ESTER project). The "Fondation Herbette—Université de Lausanne" kindly supported David Sebag during his stay at the University of Lausanne. We thank the staff of the University of Lausanne (Switzerland) for their technical and scientific supports. We are particularly grateful to Stéphanie Grand (Institute of Earth Surface Dynamics, Switzerland). We thank Alyssa Fischer (University of Neuchâtel, Switzerland) for the R script used to draw the S2 thermograms. Karin Verrecchia edited the first version of the manuscript. All authors thank the two anonymous reviewers for their constructive remarks, which substantially improved the manuscript.

SUPPLEMENTARY MATERIAL

Supplementary material for this article can be found in the online version.

CONTRIBUTION OF AUTHORS

Fabrice Bureau and Mickaël Hedde share co-last authorship.

REFERENCES

Albrecht R, Sebag D, Verrecchia E. 2015. Organic matter decomposition: Bridging the gap between Rock-Eval pyrolysis and chemical characterization (CPMAS ^{13}C NMR). *Biogeochemistry*. **122**: 101–111.

Aubert M, Bureau F, Alard D, Bardat J. 2004. Effect of tree mixture on the humic epipedon and vegetation diversity in managed beech forests (Normandy, France). *Can J Forest Res*. **34**: 233–248.

Aubert M, Hedde M, Decaëns T, Bureau F, Margerie P, Alard D. 2003. Effects of tree canopy composition on earthworms and other macroinvertebrates in beech forests of Upper Normandy (France). *Pedobiologia*. **47**: 904–912.

Aubert M, Margerie P, Ernoult A, Decaëns T, Bureau F. 2006. Variability and heterogeneity of humus forms at stand level: Comparison between pure beech and mixed beech-hornbeam forest. *Ann For Sci*. **63**: 177–188.

Aubert M, Margerie P, Trap J, Bureau F. 2010. Aboveground-belowground relationships in temperate forests: Plant litter composes and microbiota orchestrates. *For Ecol Manage*. **259**: 563–572.

Aubert M, Trap J, Chauvat M, Hedde M, Bureau F. 2018. Forest humus forms as a playground for studying aboveground-belowground relationships: Part 2, a case study along the dynamics of a broadleaved plain forest ecosystem. *Appl Soil Ecol*. **123**: 398–408.

Balesdent J, Pétraud J P, Feller C. 1991. Effets des ultrasons sur la distribution granulométrique des matières organiques des sols (Effects of ultrasound on the particle size distribution of soil organic matter). *Sci Sol* (in French). **29**: 95–106.

Barré P, Plante A F, Cécillon L, Lutfalla S, Baudin F, Bernard S, Christensen B T, Eglin T, Fernandez J M, Houot S, Kätterer T, Le Guillou C, Macdonald A, van Oort F, Chenu C. 2016. The energetic and chemical signatures of persistent soil organic matter. *Biogeochemistry*. **130**: 1–12.

Behar F, Beaumont V, De B Penteado H L. 2001. Rock-Eval 6 technology: Performances and developments. *Oil Gas Sci Technol*. **56**: 111–134.

Carrie J, Sanei H, Stern G. 2012. Standardisation of Rock-Eval pyrolysis for the analysis of recent sediments and soils. *Org Geochem*. **46**: 38–53.

Chauvat M, Trap J, Perez G, Delporte P, Aubert M. 2011. Assemblages of Collembola across a 130-year chronosequence of beech forest. *Soil Organ*. **83**: 405–418.

Delarue F, Disnar J R, Copard Y, Gogo S, Jacob J, Laggoun-Défarge F. 2013. Can Rock-Eval pyrolysis assess the biogeochemical composition of organic matter during peatification? *Org Geochem*. **61**: 66–72.

Di-Giovanni C, Disnar J R, Bichet V, Campy M. 1998. Meso-Cenozoic organic matter in present humus layers (Chaillexon basin, Doubs, France). *CR Acad Sci IIA Earth Planet Sci*. **326**: 553–559.

Disnar J R, Guillet B, Keravis D, Di-Giovanni C, Sebag D. 2003. Soil organic matter (SOM) characterization by Rock-Eval pyrolysis: Scope and limitations. *Org Geochem*. **34**: 327–343.

Durin L, Géhu J M, Noirfalise A, Sougnez N. 1967. Les hêtraies atlantiques et leur essaim climatique dans le nord-ouest et l'ouest de la France (Atlantic beech forests and their climatic cluster in northwestern and western France). *Bulletin de la Société Botanique du Nord de la France* (in French). **20**: 66–89.

Gregorich E G, Gillespie A W, Beare M H, Curtin D, Sanei H, Yanni S F. 2015. Evaluating biodegradability of soil organic matter by its thermal stability and chemical composition. *Soil Biol Biochem*. **91**: 182–191.

Hare A A, Kuzyk Z Z A, Macdonald R W, Sanei H, Barber D, Stern G A, Wang F Y. 2014. Characterization of sedimentary organic matter in recent marine sediments from Hudson Bay, Canada, by Rock-Eval pyrolysis. *Org Geochem*. **68**: 52–60.

Hedde M, Aubert M, Bureau F, Margerie P, Decaëns T. 2007. Soil detritivore macro-invertebrate assemblages throughout a managed beech rotation. *Ann For Sci*. **64**: 219–228.

Hedde M, Aubert M, Decaëns T, Bureau F. 2008. Dynamics of soil carbon in a beechwood chronosequence forest. *For Ecol Manag*. **255**: 193–202.

Hedde M, Bureau F, Chauvat M, Decaëns T. 2010. Patterns and mechanisms responsible for the relationship between the diversity of litter macro-invertebrates and leaf degradation. *Basic Appl Ecol*. **11**: 35–44.

Jabiol B, Brêthes A, Ponge J F, Toutain F, Brun J J. 2007. L'humus Sous Toutes ses Formes (Humus in Its Many Forms) (in French). ENGREF, Nancy.

Lafargue E, Marquis F, Pillot D. 1998. Rock-Eval 6 applications in hydrocarbon exploration, production, and soil contamination studies. *Rev Inst Fr Pét*. **53**: 421–437.

Lehmann J, Kleber M. 2015. The contentious nature of soil organic matter. *Nature*. **528**: 60–68.

Malou O P, Sebag D, Moulin P, Chevallier T, Badiane-Ndour N Y, Thiam A, Chapuis-Lardy L. 2020. The Rock-Eval® signature of soil organic carbon in Arenosols of the Senegalese groundnut basin. How do agricultural practices matter? *Agric Ecosyst Environ*. **301**: 107030.

Matteodo M, Grand S, Sebag D, Rowley M C, Vittoz P, Verrecchia E P. 2018. Decoupling of topsoil and subsoil controls on organic matter dynamics in the Swiss Alps. *Geoderma*. **330**: 41–51.

Peltre C, Fernandez J M, Craine J M, Plante A F. 2013. Relationships between biological and thermal indices of soil organic matter stability differ with soil organic carbon level. *Soil Sci Soc Am J*. **77**: 2020–2028.

Plante A F, Fernandez J M, Haddix M L, Steinweg J M, Conant R T. 2011. Biological, chemical and thermal indices of soil organic matter stability in four grassland soils. *Soil Biol Biochem*. **4**: 1051–1058.

Plante A F, Fernandez J M, Leifeld J. 2009. Application of thermal analysis techniques in soil science. *Geoderma*. **153**: 1–10.

Saenger A, Cécillon L, Poulenard J, Bureau F, De Daniéli S, Gonzalez J M, Brun J J. 2015. Surveying the carbon pools of mountain soils: A comparison of physical fractionation and Rock-Eval pyrolysis. *Geoderma*. **241-242**: 279–288.

Saenger A, Cécillon L, Sebag D, Brun J J. 2013. Soil organic carbon quantity, chemistry and thermal stability in a mountainous landscape: A Rock-Eval pyrolysis survey. *Org Geochem*. **54**: 101–114.

Schiedung M, Don A, Wordell-Dietrich P, Alcántara V, Kuner P, Guggenberger G. 2017. Thermal oxidation does not fractionate soil organic carbon with differing biological stabilities. *J Plant Nutr Soil Sci*. **180**: 18–26.

Schmidt M W, Torn M S, Abiven S, Dittmar T, Guggenberger G, Janssens I A, Kleber M, Kögel-Knabner I, Lehmann J, Manning D A, Nannipieri P, Rasse D P, Weiner S, Trumbore S E. 2011. Persistence of soil organic matter as an ecosystem property. *Nature*. **478**: 49–56.

Sebag D, Disnar J R, Guillet B, Di Giovanni C, Verrecchia E P, Durand A. 2006. Monitoring organic matter dynamics in soil profiles by 'Rock-Eval pyrolysis': Bulk characterization and quantification of degradation. *Eur J Soil Sci*. **57**: 344–355.

Sebag D, Verrecchia E P, Cécillon L, Adatte T, Albrecht R, Aubert M, Bureau F, Cailleau G, Copard Y, Decaëns T, Disnar J R, Hetényi M, Nyilas T, Trombino L. 2016. Dynamics of soil organic matter based on new Rock-Eval indices. *Geoderma*. **284**: 185–203.

Six J, Conant R T, Paul E A, Paustian K. 2002. Stabilization mechanisms of soil organic matter: Implications for C-saturation of soils. *Plant Soil*. **241**: 155–176.

Soucémarianadin L, Cécillon L, Guenet B, Chenu C, Baudin F, Nicolas M, Girardin C, Barré P. 2018. Environmental factors controlling soil organic carbon stability in French. *Plant Soil*. **426**: 267–286.

Thoumazeau A, Chevallier T, Baron V, Rakotondrazafy N, Panklang P, Marichal R, Kibblewhite M, Sebag D, Tivet F, Bessou C, Gay F, Brauman A. 2020. A new in-field indicator to assess the impact of land management on soil carbon dynamics. *Geoderma*. **375**: 114496.

Trap J, Bureau F, Akpa-Vinceslas M, Decaëns T, Aubert M. 2011a. Changes in humus forms and soil N pathways along a 130-year-old pure beech forest chronosequence. *Ann For Sci*. **68**: 595–606.

Trap J, Bureau F, Brethes A, Jabiol B, Ponge J F, Chauvat M, Decaëns T, Aubert M. 2011b. Does moder development along a pure beech (*Fagus sylvatica* L.) chronosequence result from changes in litter production or in decomposition rates? *Soil Biol Biochem*. **43**: 1490–1497.

Trap J, Bureau F, Perez G, Aubert M. 2013. PLS-regressions highlight litter quality as the major predictor of humus form shift along forest maturation. *Soil Biol Biochem*. **57**: 969–971.

Trap J, Laval K, Akpa-Vinceslas M, Gangneux C, Bureau F, Decaëns T, Aubert M. 2011c. Humus macro-morphology and soil microbial community changes along a 130-yr-old *Fagus sylvatica* chronosequence. *Soil Biol Biochem*. **43**: 1553–1562.

von Lützow M, Kögel-Knabner I, Ekschmitt K, Flessa H, Guggenberger G, Matzner E, Marschner B. 2007. SOM fractionation methods: Relevance to functional pools and to stabilization mechanisms. *Soil Biol Biochem*. **39**: 2183–2207.

Williams E K, Plante A F. 2018. A bioenergetic framework for assessing soil organic matter persistence. *Front Earth Sci*. **6**: 143.

Zanella A, Ponge J F, Gobat J M, Juilleret J, Blouin M, Aubert M, Chertov O, Rubio J L. 2018. Humusica 1, article 1: Essential bases—vocabulary. *Appl Soil Ecol*. **122**: 10–21.